Kidney International, Vol. 55 (1999), pp. 2349–2361

The cyclin kinase inhibitor $p21^{CIP1/WAF1}$ limits glomerular epithelial cell proliferation in experimental glomerulonephritis

YOON-GOO KIM, CHARLES E. ALPERS, JAMES BRUGAROLAS, RICHARD J. JOHNSON, WILLIAM G. COUSER, and STUART J. SHANKLAND

Departments of Medicine and Pathology, University of Washington School of Medicine, Seattle, Washington, and Howard Hughes Medical Institute, Massachusetts Institute of Technology, Cambridge, Massachusetts, USA

The cyclin kinase inhibitor $p21^{CIP1/WAF1}$ limits glomerular epithelial cell proliferation in experimental glomerulonephritis.

Background. During glomerulogenesis, visceral glomerular epithelial cells (VECs) exit the cell cycle and become terminally differentiated and quiescent. In contrast to other resident glomerular cells, VECs undergo little if any proliferation in response to injury. However, the mechanisms for this remain unclear. Cell proliferation is controlled by cell-cycle regulatory proteins where the cyclin-dependent kinase inhibitor $p21^{Cip1,WAF1}$ (p21) inhibits cell proliferation and is required for differentiation of many nonrenal cell types.

Methods. To test the hypothesis that p21 is required to maintain a differentiated and quiescent VEC phenotype, experimental glomerulonephritis was induced in p21 knockout (−/−) and p21 wild-type (+/+) mice with antiglomerular antibody. DNA synthesis (proliferating cell nuclear antigen, bromodeoxyuridine staining), VEC proliferation (multilayers of cells in Bowman's space), matrix accumulation (periodic acid-Schiff, silver staining), apoptosis (TUNEL), and renal function (serum urea nitrogen) were studied on days 5 and 14 ($N = 6$ per time point). VECs were identified by location, morphology, ezrin staining, and electron microscopy. VEC differentiation was measured by staining for Wilms' tumor-1 gene.

Results. Kidneys from unmanipulated p21−/− mice were histologically normal and did not have increased DNA synthesis, suggesting that p21 was not required for the induction of VEC terminal differentiation. Proliferating cell nuclear antigen and bromodeoxyuridine staining was increased 4.3- and 3.3-fold, respectively, in p21−/− mice with glomerulonephritis ($P < 0.0001$ vs. p21+/+ mice). At each time point, VEC proliferation was also increased in nephritic p21−/− mice ($P < 0.0001$ vs. p21+/+ mice). VEC re-entry into the cell cycle was associated with the loss of Wilms' tumor-1 gene staining. Nephritic p21−/− mice had increased extracellular matrix protein accumulation and apoptosis and decreased renal function (serum urea nitrogen) compared with p21+/+ mice ($P < 0.001$).

Conclusion. These results show that the cyclin kinase inhibitor p21 is not required by VECs to attain a terminally differentiated VEC phenotype. However, the loss of p21, in disease states, is associated with VEC re-entry into the cell cycle and the development of a dedifferentiated proliferative phenotype.

Key words: glomerulus, podocyte, cell cycle, kidney, p21, cyclin dependent kinase, visceral glomerular epithelial cells, injury.

Received for publication November 6, 1998
and in revised form February 1, 1998
Accepted for publication February 4, 1998

Glomerular endothelial and mesangial cells proliferate in many forms of glomerular disease [1]. In contrast, the visceral glomerular epithelial cell (VEC) or podocyte does not readily proliferate in response to injury [2, 3]. Thus, in diseases of the VEC, such as minimal change, membranous nephropathy, and focal glomerulosclerosis, VEC proliferation has not been detected. However, in diseases such as HIV or collapsing glomerulopathy, VEC hypercellularity has been demonstrated [4]. Although many authorities believe that the lack of VEC proliferation *in vivo* is because this cell type is terminally differentiated, the determinants of VEC proliferation have not yet been fully elucidated, and it remains unclear why VECs proliferate in some but not all forms of glomerular injury.

Cell proliferation is controlled at the nuclear level by cell-cycle regulatory proteins [5]. Progression through the cell cycle requires that cyclin-dependent kinases (CDKs) be activated by partner cyclins [6, 7]. CDKs are negatively regulated by cyclin-kinase inhibitors (CKIs), which inhibit cell proliferation by causing cell-cycle arrest [8]. Two families of CKIs have been identified based on sequence homology and their target cyclin-CDK complexes that are inhibited [8]. The INK4 family of CKIs, p15, p16, p18, p19, inhibit G1 CDKs. The CIP/KIP family of CKI, which includes $p21^{CIP1,WAF1}$ (p21) [9–12], $p27^{Kip1}$ (p27) [13, 14], and $p57^{Kip2}$ (p57) [15], share homology at the amino terminus and inhibit G1- and S-phase cyclin-CDK complexes. Only p21 binds to and inhibits the proliferating cell nuclear antigen (PCNA) through its carboxy terminus [16, 17]. Furthermore, p21 exists in quaternary complexes that contain cyclin, CDKs, and PCNA in normal cells [18]. In contrast to other members of this family of CKIs, p21 is transcriptionally regulated

through p53-dependent [11] and p53-independent pathways [19].

We have recently shown that p21 expression is increased in response to immune-mediated injury to the VECs in the passive Heymann nephritis (PHN) model of membranous nephropathy and is associated with an increase in DNA synthesis but not proliferation [20]. Furthermore, giving the mitogen basic fibroblast growth factor to PHN rats decreases p21 expression, which is associated with increased DNA synthesis [20]. In this study, we tested the postulate that p21 is required to maintain a differentiated and quiescent VEC phenotype. Our results show that glomerular epithelial cell proliferation was greatly increased in p21−/− mice with experimental glomerulonephritis, evidence strongly in favor of this hypothesis, and that this was associated with increased matrix production and decreased renal function.

METHODS

Animal model of experimental glomerulonephritis

Experimental glomerulonephritis was induced in p21 knockout (p21−/−) and p21 wild-type (p21+/+) mice aged 14 ~ 20 weeks (weight 28 ~ 38 g) with a sheep antibody to rabbit glomeruli (0.5 ml/20 g body wt intraperitoneal injections per day for two consecutive days). Briefly, rabbit glomeruli for immunization were isolated by differential sieving techniques and contained less than one tubular fraction per 100 glomeruli. Sheep antirabbit glomerular antibody was produced in a sheep immunized three to four times at two-week intervals with lyophilized whole rabbit glomeruli emulsified in complete Freund's adjuvant at the first immunization and in incomplete Freund's adjuvant at later immunizations. Antisera were heat inactivated at 56°C for 30 minutes, and immune IgG was isolated by using caprylic acid.

p21−/− and p21+/+ mice [21] were sacrificed at day 5 and day 14 ($N = 6$ at each time point per group) after the second injection of antiglomerular antibody. Unmanipulated age-matched p21+/+ and p21−/− mice served as normal controls ($N = 6$ in each group). Renal function was assessed by urine protein excretion and serum urea nitrogen level. Urine from each animal was collected for 24 hours prior to sacrifice, and protein excretion was quantitated by the sulfosalicylic acid method. Blood samples were also obtained at sacrifice for serum urea nitrogen measurement as previously described [22]. To measure DNA synthesis, each animal was injected with bromodeoxyuridine (BrdU; cell proliferation kit; 1 ml/100 g body wt; Amersham Life Science, Arlington Heights, IL, USA) intraperitoneally two hours before sacrifice. Kidney biopsies were fixed in formalin, methyl Carnoy's solution, OCT, and half-strength Karnofskys. All animal studies were performed in an accredited animal care facility in accord with the National Institutes of Health guidelines for the Care and Use of Laboratory Animals.

Immunostaining

Immunofluorescence staining. To ensure that the glomerular deposition of the sheep antiglomerular antibody was similar in p21−/− and p21+/+ mice, tissues from normal and diseased mice were embedded in OCT Compound (Miles, Elkart, IN, USA) and rapidly snap frozen in isopentane in liquid nitrogen as previously described [23]. Four-micrometer-thick frozen sections were stained with fluorescein isothiocyanate-conjugated antibodies to sheep IgG and mouse C3 (Cappel, Durham, NC, USA). To measure the autologous phase of the immune response, immunostaining was also performed with fluorescein isothiocyanate-conjugated antibodies to mouse IgG (Cappel). Staining was quantitated on 50 consecutive glomeruli and graded 0 to 4+ based on the intensity of the staining and the percentage of glomerular surface area that stained, as described elsewhere [24]. To determine if fibrinogen was increased in this model, staining was performed with an antibody to mouse fibrinogen (Cappel).

Assessment of glomerular cell proliferation. Glomerular cell proliferation was measured by the following methods. (*1*) PAS stain. Four-micrometer-thick methyl carnoys fixed sections were stained with periodic acid-Schiff reagent (PAS) or methenamine-silver to measure glomerular cell proliferation, which was classified based on the number of cell layers in Bowman's space: (*a*) mild proliferation was defined as two layers of cells, and (*b*) severe proliferation was defined as three or more layers of cells occupying Bowman's space. To measure the percentage of glomeruli with these changes, a minimum of 50 glomeruli from each animal were examined. The percentage of mild and severe proliferation was also recorded in each animal. (*2*) PCNA staining (a marker of DNA synthesis) with a murine monoclonal antibody to PCNA (19A2; Coulter Immunology, Hialeah, FL, USA; immunoperoxidase staining is discussed later in this article). (*3*) BrdU staining (a marker of DNA synthesis) with a murine monoclonal antibody to BrdU (immunoperoxidase staining is also discussed later; Amersham Life Science).

Identification of proliferating glomerular cell type. The following methods were used to determine which glomerular cell type underwent DNA synthesis and which cell type proliferated to make up the multilayers of cells in Bowman's space. (*a*) The first was ezrin staining with a rabbit polyclonal antibody to ezrin (gift from Heinz Furthmayr, Stanford University School of Medicine, Stanford, CA, USA), which is expressed on visceral and parietal glomerular epithelial cells, as previously described and utilized [25]. (*b*) To determine the presence of infiltrating cells, rat monoclonal antibodies to mouse

neutrophils (clone 7/4; Catalag Laboratories, Burlingame, CA, USA), macrophages (F4/80; Catalag), T-lymphocyte CD4 and CD8 antigens (immunoperoxidase staining on acetone fixed frozen tissue sections; Catalag) were used. Mouse spleen served as a positive control. (*c*) Rabbit polyclonal antibody to Wilms tumor-1 gene (Santa Cruz Biotechnology, Santa Cruz, CA) was a marker of differentiated VEC [26]. (*d*) The glomerular cell type undergoing DNA synthesis was also determined by double immunostaining for BrdU and ezrin (discussed later in this article). (*e*) To ensure that the proliferating cell type was not proximal tubule, immunostaining was performed with an antibody to rat proximal tubular brush border (anti-Fx1A) [27]. (*f*) To define better which glomerular cell type was involved at an ultrastructural level, tissues were fixed in half-strength Karnofsky's solution (1% paraformaldehyde and 1.25% glutaraldehyde in 0.1 M Na cacodylate buffer, pH 7.0), postfixed in osmium tetroxide, dehydrated in graded ethanol, and embedded in epoxy resin, and electron microscopy was performed. Thin sections were stained with uranyl acetate and lead citrate and examined with a Philips 410 (Philips Export BV, Eindhoven, The Netherlands) electron microscope.

Single indirect immunoperoxidase staining. This was performed on 4 μm sections of methyl Carnoy's fixed kidney tissues as previously described with the primary antibodies listed earlier here. For BrdU staining, tissue sections were boiled in a microwave for 10 minutes in 0.01 M sodium citrate buffer, pH 6.0, and staining was performed according to the manufacturer's instructions (Amersham Proliferation Kit; Amersham). For all immunostains, primary antibodies were incubated overnight at 4°C, followed by a biotinylated secondary antibody incubated for 30 minutes at room temperature and a horseradish peroxidase-conjugated avidin D at room temperature for 20 minutes. Brown cytoplasmic staining was detected with diaminobenzidine (DAB), and black nuclear staining (PCNA, BrdU) was detected with nickel as a chromogen. Controls included omitting the primary antibody and substituting the primary antibody with an irrelevant antibody of the same IgG class.

Double-immunostaining. Sections were first stained for BrdU using nickel as a chromagen, followed by the antibody to ezrin, which was detected with the vectastain ABC-AP kit using vector red (Vector Laboratories, Burlingame, CA, USA) as a chromagen.

Quantitation of immunostaining for each antibody was performed on more than 50 glomeruli from each animal in a blinded fashion. Results were reported as the number of positive staining cells per glomerular cross section ± SEM.

Assessment of glomerulosclerosis. Glomerulosclerosis was measured on silver-stained sections and was graded quantitatively based on the percentage of glomerular tuft area involvement as follows: grade 0 = normal glomerulus; grade 1 = sclerosis involved less than 25% of glomerular tuft area; grade 2 = sclerosis involving 25 to 50%; grade 3 = sclerosis involving 50 to 75%; and grade 4 = sclerosis involving 75 to 100% of glomerular tuft area. A minimum of 50 glomeruli were evaluated in individual animals, and the mean score ± SEM was reported.

Table 1. Serum urea nitrogen (mg/dl) in normal mice and at days 5 and 14 of glomerulonephritis

	Normal	Day 5	Day 14
$p21^{-/-}$ mice	53.6 ± 9.6	140.1 ± 24.6[a]	243.8 ± 9.3[a,b]
$p21^{+/+}$ mice	53.0 ± 2.5	153.6 ± 13.1[a]	127.7 ± 24.9[a]

Values are mean ± SE.
[a] $P < 0.01$ vs. normal in each group
[b] $P = 0.0012$ vs. $p21^{+/+}$ mice at day 14

Measuring apoptosis. To measure DNA nicking, a marker of apoptosis, the TUNEL assay was performed on formalin-fixed tissue as previously described [20, 28]. Terminal deoxynucleotidyl transferase (TdT) was omitted from the nucleotide mixture as a negative control. Tissue sections treated with DNAse to introduce DNA breaks in all nuclei were used as positive controls. Quantitation of TUNEL staining was performed on more than 50 glomeruli from each animal in a blinded fashion. Results were reported as the number of positive TUNEL staining cells ± SEM per glomerular cross section.

Statistical analysis

The Mann–Whitney *U*-test was used for statistical analysis. All values were expressed as mean ± SEM. A *P* value of less than 0.05 was considered statistically significant.

RESULTS

Baseline p21−/− mice kidneys are normal

The phenotype of p21−/− mice used in this study has been previously reported as normal [21]. Our study showed that p21−/− and p21+/+ mice not exposed to antibody (normal controls) had normal renal function, as measured by serum urea nitrogen (Table 1) and urine protein excretion. The renal histology in control p21−/− and p21+/+ mice was normal by light (results not shown) and electron microscopy (results not shown). There was also no staining for mouse IgG and C3, indicating that no spontaneous glomerular antibody deposition occurred in these mice.

Antibody deposition was similar in p21−/− and p21+/+ mice

Glomerular immunofluorescence staining was present for sheep IgG, mouse IgG, and C3 in all glomeruli in

both p21+/+ and p21−/− mice at days 5 and 14 of disease, and there was no quantitative difference at any time point in staining for these antigens in p21−/− and p21+/+ mice ($P > 0.05$, data not shown). These results show that both antiglomerular antibody deposition and the autologous phase immune response were similar in p21+/+ and p21−/− mice.

Light microscopy

The histological patterns of injury in p21+/+ mice and p21−/− mice were similar (Fig. 1 A, B). However, the extent and severity of injury were clearly greater in p21−/− mice by day 14 of injury compared with p21+/+ controls. The glomerular lesion consisted of varying degrees of capillary collapse, with patterns ranging from segmental distribution to global involvement of glomeruli (Fig. 1 A, B). The most severely affected glomeruli showed complete or near complete loss of identifiable capillary lumina with relative prominence of the mesangial area because of collapsed matrices and cellular accumulation (Fig. 1E). Numerous preserved capillary loops in severely injured glomeruli contained occlusive intensely PAS stained material, that also stained positive for fibrin (not shown), characteristic of microthrombi. Such severely injured glomeruli were widespread in p21−/− mice at day 14 of the injury process (Fig. 1E) and were only occasionally encountered in either p21−/− or p21+/+ mice at day 5 of the injury process.

In the most mildly injured glomeruli, seen most often at day 5 in p21−/− mice, the histological alterations were limited to vacuolization of both visceral and parietal epithelial cells (Fig. 1 A, B). Glomeruli with an injury ranging from mild to severe also showed accumulations of swollen cells within the urinary (Bowman's) space adjacent to glomerular capillary loops with staining and structural appearances similar to both visceral and parietal epithelial cells (Fig. 1 A, B, E). Sometimes these cellular accumulations were limited to clusters of as few as four to five cells adjacent to a capillary within a single histological plane of section; other times they formed cell clusters of 10 or more cell bodies, at times filling the urinary space with an appearance indistinguishable from a cellular crescent (Fig. 1 E, F).

Cells in Bowman's space were classified based on the number of cell layers in Bowman's space into mild (≤ 2) and severe (≥ 3) (Fig. 2). At day 5, there was no significant difference in the number of glomeruli with multilayered cell layers in Bowman's space in p21−/− mice and p21+/+ mice (Fig. 2), although there was a trend toward more severe proliferation in p21−/− mice (21.7 ± 2.0 vs. 15.8 ± 5.5%, $P > 0.05$; Fig. 2). In contrast, at day 14, the percentage of glomeruli with multilayered cells was 2.4-fold higher in p21−/− mice compared with p21+/+ mice (Fig. 2). Furthermore, at day 14 in p21−/− mice, the majority of glomeruli with cell proliferation were classified as severe.

Tubulointerstitial changes consisted of tubular dilation, intraluminal tubular casts and widening of the interstitial space accompanied by accumulation of interstitial leukocytes (results not shown). The severity of these changes closely paralleled the extent of injury manifest by glomeruli. Arterial vessels were without demonstrable histological abnormalities in all of the study groups.

Electron microscopy

Both p21−/− and control mice exhibited striking evidence of thrombotic microangiopathy (TMA), which was evident by ultrastructural examination at both day 5 and 14 (Fig. 3), but which was evident only to a much lesser degree in histological section. Characteristic features of TMA included occlusion of glomerular capillaries by thrombus, focal entrapment of leukocytes and erythrocytes within thrombi, and widespread dissolution of the compact mesangial matrix (mesangiolysis) in mesangial areas adjacent to thrombosed capillaries. In some glomeruli without overt thrombi, circulating platelets were also prominent within capillary lumina.

Glomerular basement membranes had no identifiable abnormalities. In glomeruli or segments of glomeruli without thrombi, VECs demonstrated extensive effacement of foot processes (Fig. 3). Specific abnormalities of VEC bodies in these areas were not identified. An examination of cells within Bowman's space indicated the great majority were most consistent with an epithelial cell phenotype. These cells demonstrated features of focally abundant rough endoplasmic reticulum, numerous mitochondria, occasionally well-developed Golgi apparatus, and relative paucity of lysosomes and granules such as those found in nearby intracapillary leukocytes.

Fig. 1. Light micrographs of nephritic kidneys at day 5. In both p21+/+ (*A*) and p21−/− (*B*) mice, there was vacuolization, detachment, and cyst formation of the visceral glomerular epithelial cells (VECs). PAS-positive material occluded many of the capillary loops, which were associated with capillary collapse, and this was more extensive in the p21−/− mice (B). (*C* and *D*) BrdU staining. BrdU staining was increased at day 5 in nephritic p21−/− (D) mice compared with nephritic p21+/+ (C) mice, and the pattern of BrdU staining was predominantly in a VEC distribution. (*E*) PAS stain of nephritic p21−/− at day 14. There was an occlusion of capillaries and a collapse of the glomerular tuft. Layers of cells filled Bowman's space, and these were in a typical VEC distribution. (*F*) Ezrin stain. Layers of cells in p21−/− mice at day 14 stained positive for Ezrin, a marker of glomerular epithelial cells.

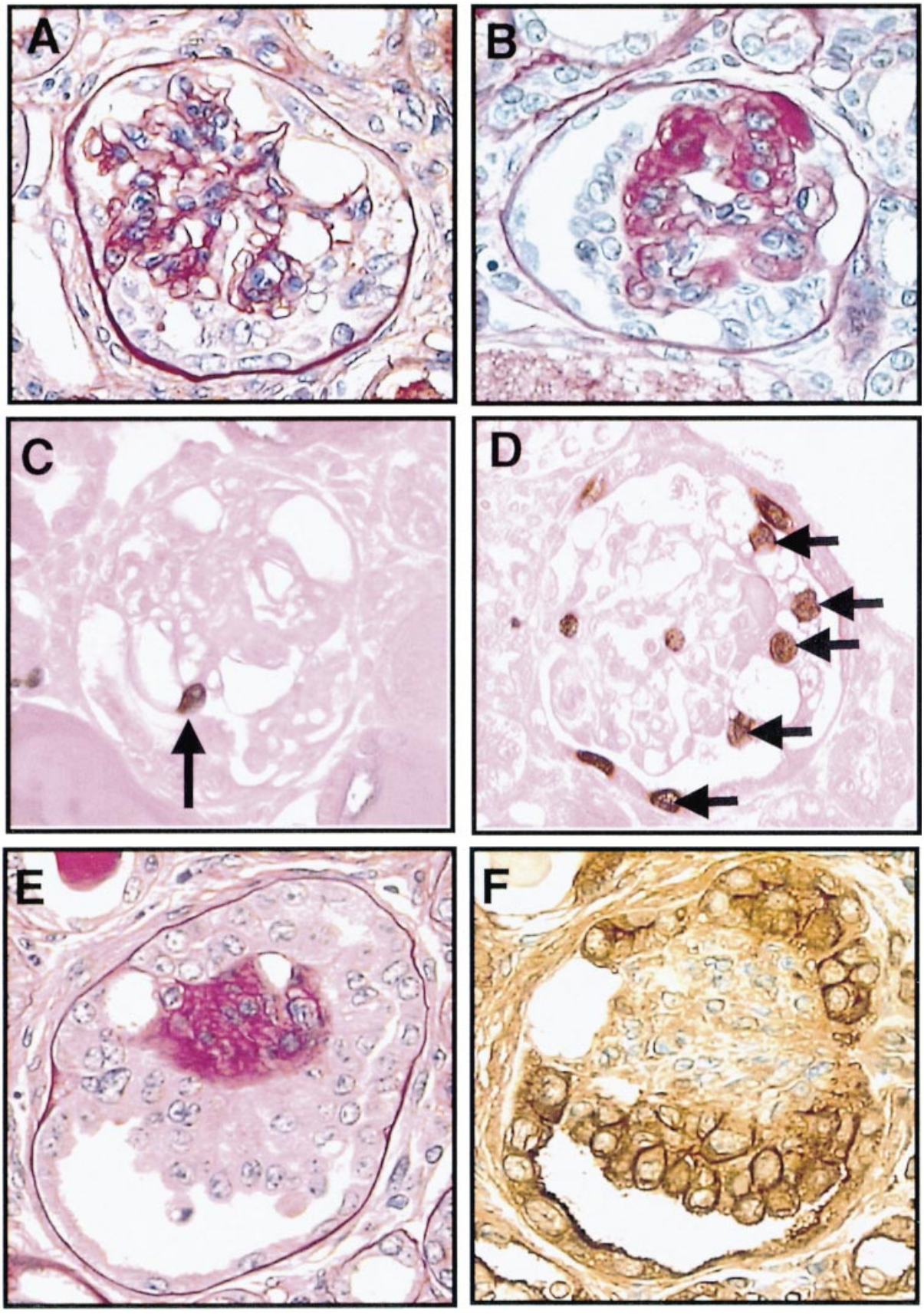
A
B
C
D
E
F

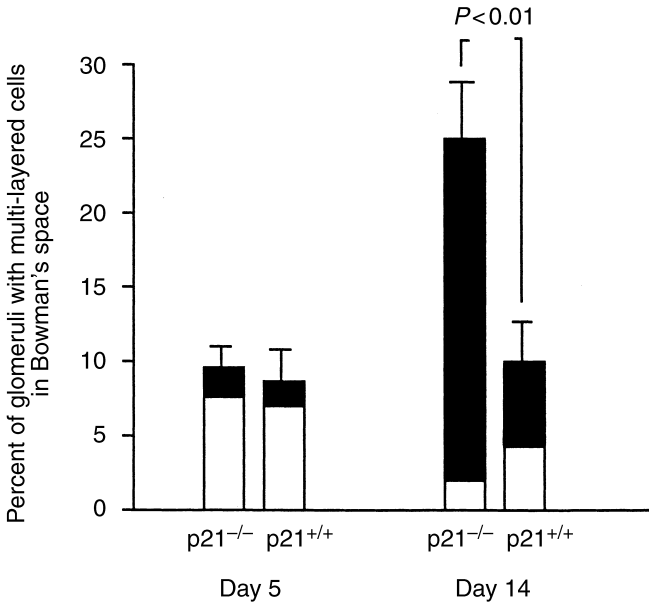

Fig. 2. Quantitation of glomerular cell proliferation. Glomerular cell proliferation was measured by the percentage of glomeruli with cell multilayers, which was classified as mild (<3 layers; □) or severe (≥3 layers; ■). There was no significant difference in the number of multilayered cells at day 5 of glomerulonephritis between p21+/+ and p21−/− mice. At day 14, glomerular cell proliferation increased in nephritic p21−/− mice compared with controls, where the majority of cell multilayers were severe.

In the most severely injured glomeruli, there were numerous areas of complete detachment of VEC foot processes from the capillary basement membranes in addition to foci of foot process effacement. Cells within the urinary space, although focally numerous, had a predominately epithelial phenotype as described earlier here (Fig. 3). Although these cells frequently had closely opposed cell bodies, discrete cell attachment sites, such as zona occludens, were not identified.

DNA synthesis increased in nephritic p21−/− mice

DNA synthesis was measured by immunostaining for PCNA and BrdU (Fig. 1 C, D) and was not detected in the glomeruli of normal p21−/− and p21+/+ mice prior to being injected with the sheep antirabbit antibody (Fig. 4). Thus, the loss of p21 by itself was not sufficient to induce DNA synthesis or increase glomerular cell number under normal physiological conditions.

Glomerular immunostaining for PCNA and BrdU (Fig. 1 C, D) was increased in p21+/+ mice at day 5 of glomerulonephritis compared with normal p21+/+ mice (Fig. 1 C, D, and Fig. 4). However, glomerular immunostaining for PCNA was 1.8-fold greater in p21−/− mice at day 5 compared with p21+/+ mice ($P = 0.0002$; Fig. 4A). Similarly, the number of glomerular cells staining positive for BrdU was 2.3-fold greater in p21−/− mice at day 5 compared with p21+/+ mice ($P = 0.002$; Fig. 4B).

At day 14 of glomerulonephritis, glomerular immunostaining for PCNA was 4.3-fold greater in p21−/− mice compared with p21+/+ mice ($P = 0.0002$; Fig. 4A), and glomerular staining for BrdU was 3.3-fold increased in p21−/− mice compared with p21+/+ mice ($P = 0.001$; Fig. 4B). Thus, DNA synthesis was significantly increased at all time points in p21−/− mice following immune-mediated glomerular injury compared with p21+/+ mice. At both days 5 and 14, cells staining positively for PCNA and BrdU (Fig. 1 C, D) were in a typical VEC distribution. Furthermore, PCNA- and BrdU-positive cells had the typical morphological appearance of VECs on light microscopy.

Proliferating cell type is predominantly visceral glomerular epithelial cells in nephritic p21−/− mice

We used several methods to determine which glomerular cell type(s) was proliferating in this model. In nephritic p21+/+ mice, proliferation was confined to both visceral and parietal glomerular epithelial cells. In contrast, in nephritic p21−/− mice, the overwhelming cell type proliferating was VEC, based on the following evidence. First, the multilayered cells in the glomeruli had the typical morphological appearance and distribution on PAS staining of VEC (Fig. 1 E, F). Second, electron microscopy showed that VECs were vacuolated, swollen, and detached, which is suggestive of VEC injury (Fig. 3). Third, staining for macrophages, neutrophils, and CD4 and CD8 lymphocytes was not detected in the glomeruli of p21−/− and p21+/+ mice (Table 2), suggesting that it was unlikely that these infiltrating cells made up the multilayered cell structures in Bowman's space. Fourth, staining for the tubular brush border was limited to the proximal tubules and was not detected in glomerular multilayered cell structures (results not shown). Fifth, although ezrin stains both visceral and parietal epithelial cells, double immunostaining showed that the vast majority (more than 95%) of PCNA- and BrdU-positive cells were also ezrin positive ($PCNA^+/ezrin^+$; $BrdU^+/ezrin^+$), and staining for ezrin and PAS on serial sections showed that the majority (more than 95%) of cells in the multicell layers that stained positive for ezrin had the appearance of typical VECs (Fig. 1F). These data show that the predominant cell type undergoing DNA synthesis and proliferation in nephritic p21−/− were VECs, whereas both visceral and parietal epithelial cells proliferated in nephritic p21+/+ mice.

Proliferating visceral glomerular epithelial cells lose Wilms' tumor-1 gene staining

Wilms' tumor-1 gene is expressed constitutively in normal VECs and is a marker of mature differentiated VECs [26]. Figure 5 shows that Wilms' tumor-1 gene (WT-1) immunostaining was detected in normal p21−/− mice in a typical VEC distribution. However, in nephritic

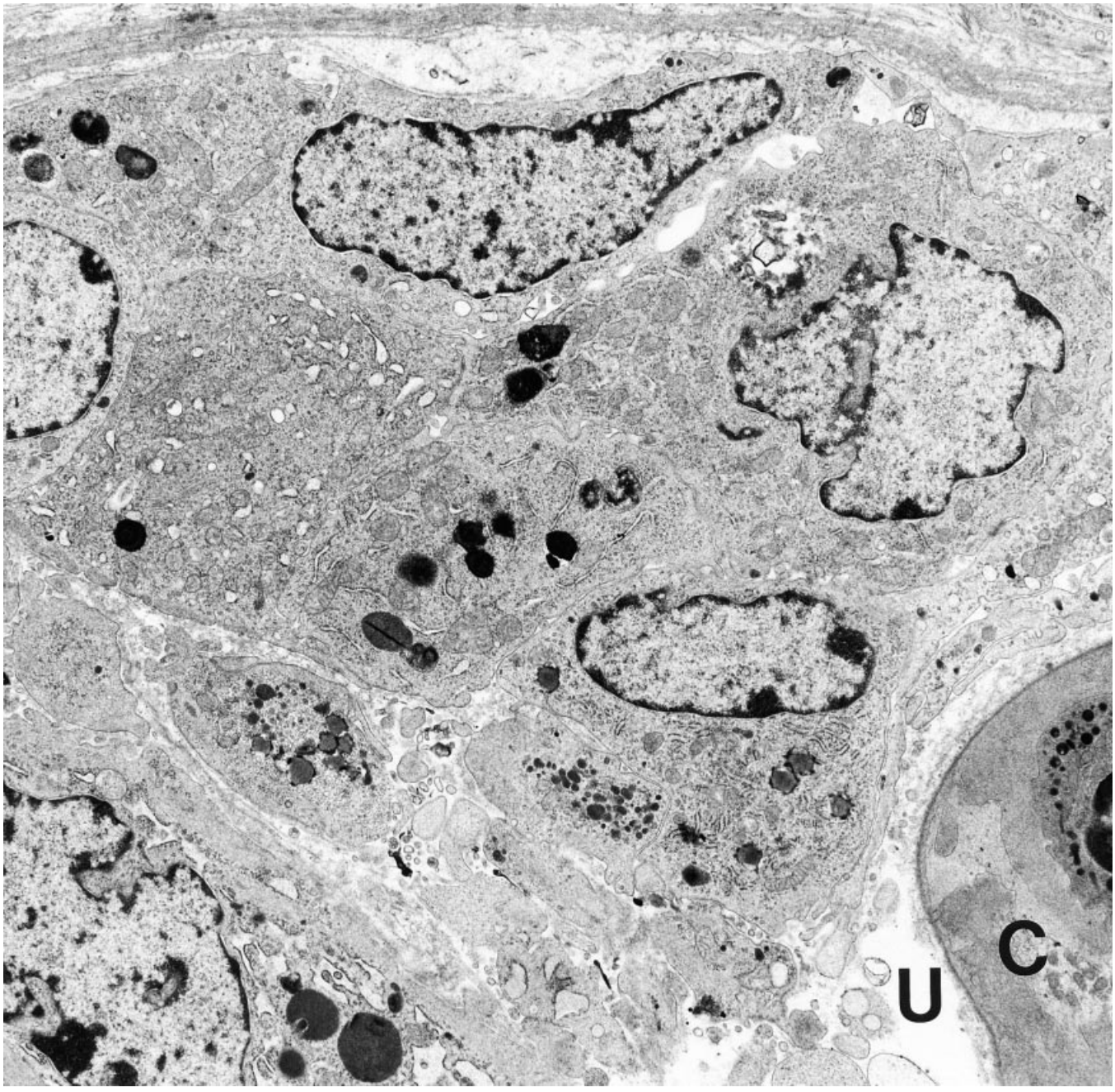

Fig. 3. Electron micrograph of part of a glomerulus from day 14 p21−/− mouse. A capillary loop (C, lower right) is occluded by thrombus and contains part of a leukocyte with numerous cytoplasmic granules. The adjacent urinary space contains clusters of cells showing few cytoplasmic granules prominent rough endoplasmic reticulum and numerous mitochondria. Discrete intercellular junctions between these cells cannot be identified.

p21−/− mice, VEC immunostaining for WT-1 decreased at day 5, which coincided with increased DNA synthesis. Furthermore, WT-1 staining was not detected in glomeruli with multilayered cells at day 14 (Fig. 5) in p21−/− mice. These results show that proliferating VECs have lost a feature that characterizes their differentiated phenotype.

Glomerulosclerosis was increased in nephritic p21−/− mice

Glomerulosclerosis was quantitated on silver-stained sections (Fig. 6 A, B). Silver staining increased at day 5 in both p21+/+ and p21−/− mice, but the difference did not reach statistical difference between mice strains at this time point (0.20 ± 0.04 vs. 0.33 ± 0.15, $P >$

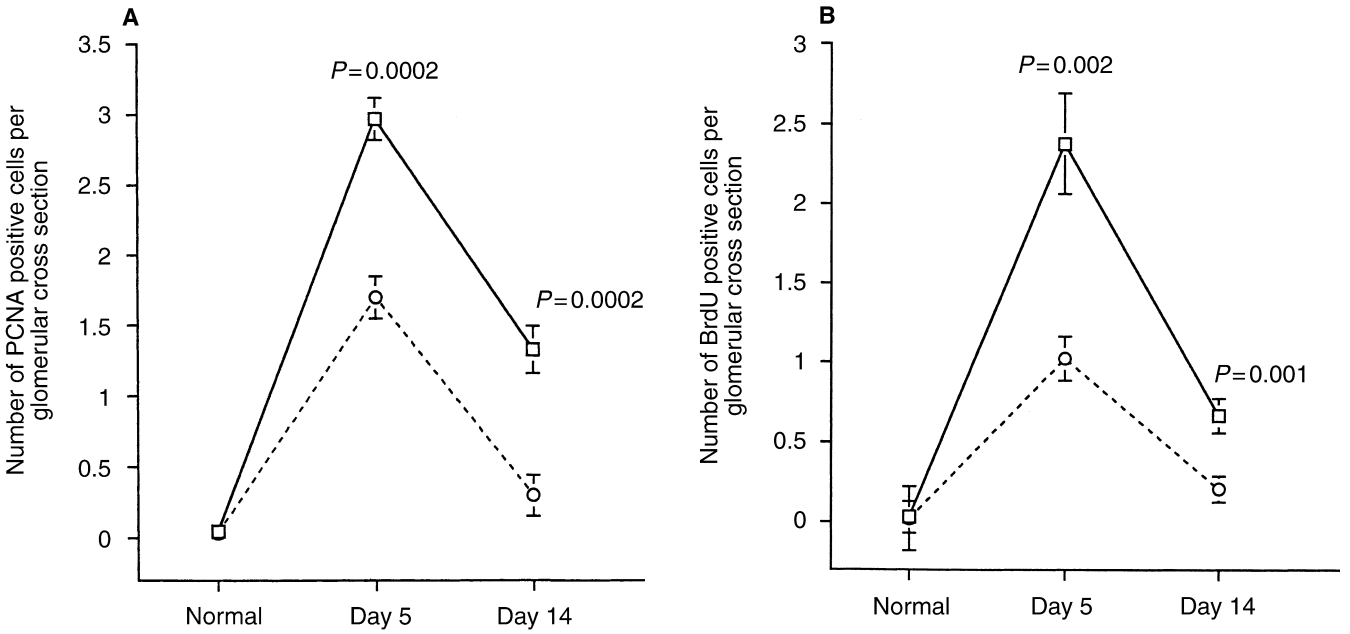

Fig. 4. Quantitation of DNA synthesis. DNA synthesis was measured by immunostaining for proliferating cell nuclear antigen (PCNA; *A*) and bromodeoxyuridine (BrdU; *B*). PCNA and BrdU staining was not detected in normal control p21+/+ (○) and p21−/− (□) mice. DNA synthesis increased significantly in nephritic p21−/− mice at day 5 and 14 compared with p21+/+ mice.

Table 2. Quantitation of glomerular immunostaining for infiltrating cells in normal and nephritic mice showing that infiltrating cells did not make up the multilayers of cells in Bowman's space

	Normal		Day 5		Day 14	
	$p21^{-/-}$	$p21^{+/+}$	$p21^{-/-}$	$p21^{+/+}$	$p21^{-/-}$	$p21^{+/+}$
Leukocytes	0.152 ± 0.033	0.150 ± 0.024	0.108 ± 0.024	0.173 ± 0.041	0.090 ± 0.027	0.083 ± 0.016
Macrophages	0.013 ± 0.007	0.007 ± 0.007	0.072 ± 0.020	0.080 ± 0.007	0.160 ± 0.051	0.093 ± 0.019
CD4+ T-cells	0.013 ± 0.007	0.013 ± 0.007	0.016 ± 0.007	0.013 ± 0.007	0.023 ± 0.013	0.020 ± 0.007
CD8+ T-cells	0.013 ± 0.013	0.007 ± 0.007	0.020 ± 0.009	0.013 ± 0.007	0.017 ± 0.008	0.020 ± 0.005

Values are expressed as mean number of cells ± SE per glomerular cross section.

0.05). In contrast, at day 14, the glomerulosclerosis score was 1.7-fold increased in p21−/− mice compared with p21+/+ (1.29 ± 0.13 vs. 0.74 ± 0.10, $P = 0.0009$).

Glomerular apoptosis was increased in nephritic p21−/− mice

Apoptosis was measured by TUNEL immunostaining (Fig. 6 C, D, and Fig. 7). Glomerular TUNEL staining was not detected in normal p21−/− and p21+/+ mice (Fig. 7). Although there was a slight increase in TUNEL staining at day 5 of glomerulonephritis in p21−/− and p21+/+ mice compared with normal, TUNEL staining was not different between the two groups (Fig. 7). In contrast, TUNEL staining was 3.8-fold greater in p21−/− mice at day 14 compared with p21+/+ mice (1.11 ± 0.08 vs. 0.29 ± 0.79 per glomerular tuft area, $P < 0.0001$; Fig. 6 C, D and Fig. 7).

Renal function was decreased in p21−/− mice with glomerulonephritis

Serum urea nitrogen increased in both p21−/− and p21+/+ mice at day 5 and 14 of glomerulonephritis (Table 1), but was higher by a factor of two in p21−/− mice compared with p21+/+. Urine protein excretion was not increased at day 14 (16.2 ± 2.5 vs. 17.2 ± 3.6 mg/24 hr, $P > 0.05$) in either group.

DISCUSSION

In this study, we show that VEC DNA synthesis and proliferation leading to multilayers of VECs in Bowman's space, sometimes resembling crescents in appearance, are increased in p21−/− mice with experimental immune-mediated glomerulonephritis. We demonstrate that this VEC proliferation was associated with increased glomerulosclerosis and decreased renal function.

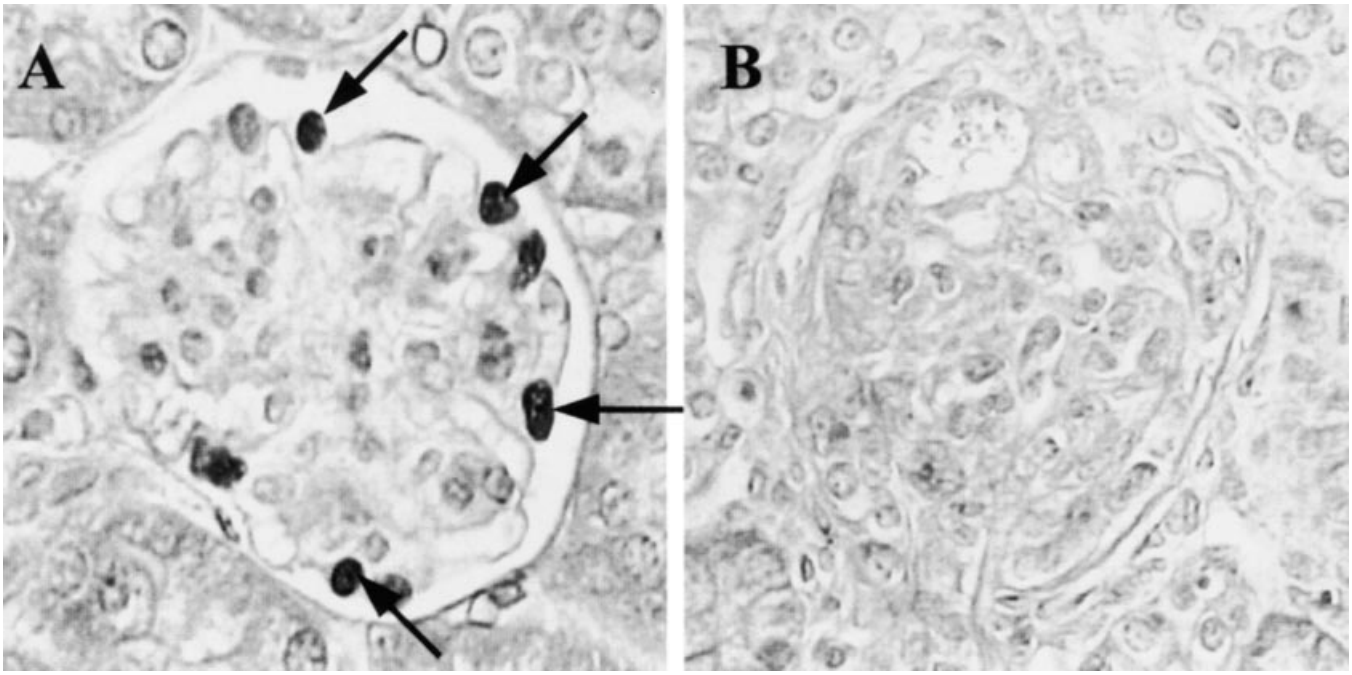

Fig. 5. Indirect immunoperoxidase immunostaining for Wilms' tumor-1 gene (WT-1) in p21−/− mice. (*A*) Glomerular cells stain positive for WT-1 in normal p21−/− mice, and this is in a visceral glomerular epithelial cell distribution (arrows). (*B*) WT-1 staining was not detected in glomerular cell multilayers in p21−/− mice with glomerulonephritis at day 14.

The cyclin kinase inhibitor p21 is complexed with cyclins, CDKs, and PCNA in normal cells *in vitro* [18, 29]. There are several lines of evidence to show that p21 limits proliferation *in vitro* and *in vivo*. Forced overexpression of p21 inhibits G1/S transition and arrests the cell cycle in renal [30] and nonrenal cells [11]. Proliferation is increased in fibroblasts when cellular p21 levels are lowered with antisense oligonucleotides [31], and the response to mitogens is increased in keratinocytes from p21−/− mice *in vitro* [32]. In addition, a role for p21 has also been demonstrated in nonrenal cell differentiation where p21 expression is induced during embryogenesis and correlates with cell cycle arrest [33]. The correlation of terminal differentiation with p21 induction has also been demonstrated *in vitro* [34–36].

Visceral glomerular epithelial cells proliferate during the S phase of glomerulogenesis and exit the cell cycle during the capillary loop phase, where they acquire a highly specialized, quiescent, and terminally differentiated cell type [37]. In accord with other organs studied in these mice [32, 38], the first finding in this study was that the kidneys of p21−/− mice were normal and that glomerular DNA synthesis and cell number were not increased under normal physiological conditions. In contrast, the loss of p57 is associated with abnormal VEC development, and VECs from p57 null mice are born with a fused foot process [15]. In human development, there is a *de novo* expression of p27 in VECs, and this coincides with VEC exit from the cell cycle and the acquisition of a terminally differentiated phenotype [39]. The data in this study suggest that p21 is not required for VEC exit from the cell cycle and the induction of VEC terminal differentiation during glomerulogenesis and that the loss of p21 by itself was not sufficient to increase glomerular cell proliferation. Thus, p21 is not essential for normal glomerular development.

In this study, we showed that staining for PCNA and BrdU, markers of DNA synthesis, increased in p21−/− mice with glomerulonephritis compared with p21+/+ mice. Moreover, the increased VEC number was associated with the formation of multilayered structures, sometimes resembling glomerular crescents. Thus, a second major finding in this study was that following immune-mediated injury, VECs re-engage the cell cycle and undergo marked DNA synthesis and proliferation in the absence of the cyclin kinase inhibitor p21. The increase in VEC number indicates that these cells do not exhibit a block in cytokinesis, which is a mechanism that has been proposed to underlie the inability of VECs to proliferate [40]. In the PHN model of immune-mediated VEC injury, there is a *de novo* expression of p21 in VECs, and p21 was complexed to and inhibited the activity of cyclin A-CDK2 [20]. This was accompanied by only low-grade DNA synthesis of VECs. Interestingly, injecting the mitogen basic fibroblast growth factor to PHN rats decreased p21, but not p27 expression, and this was ac-

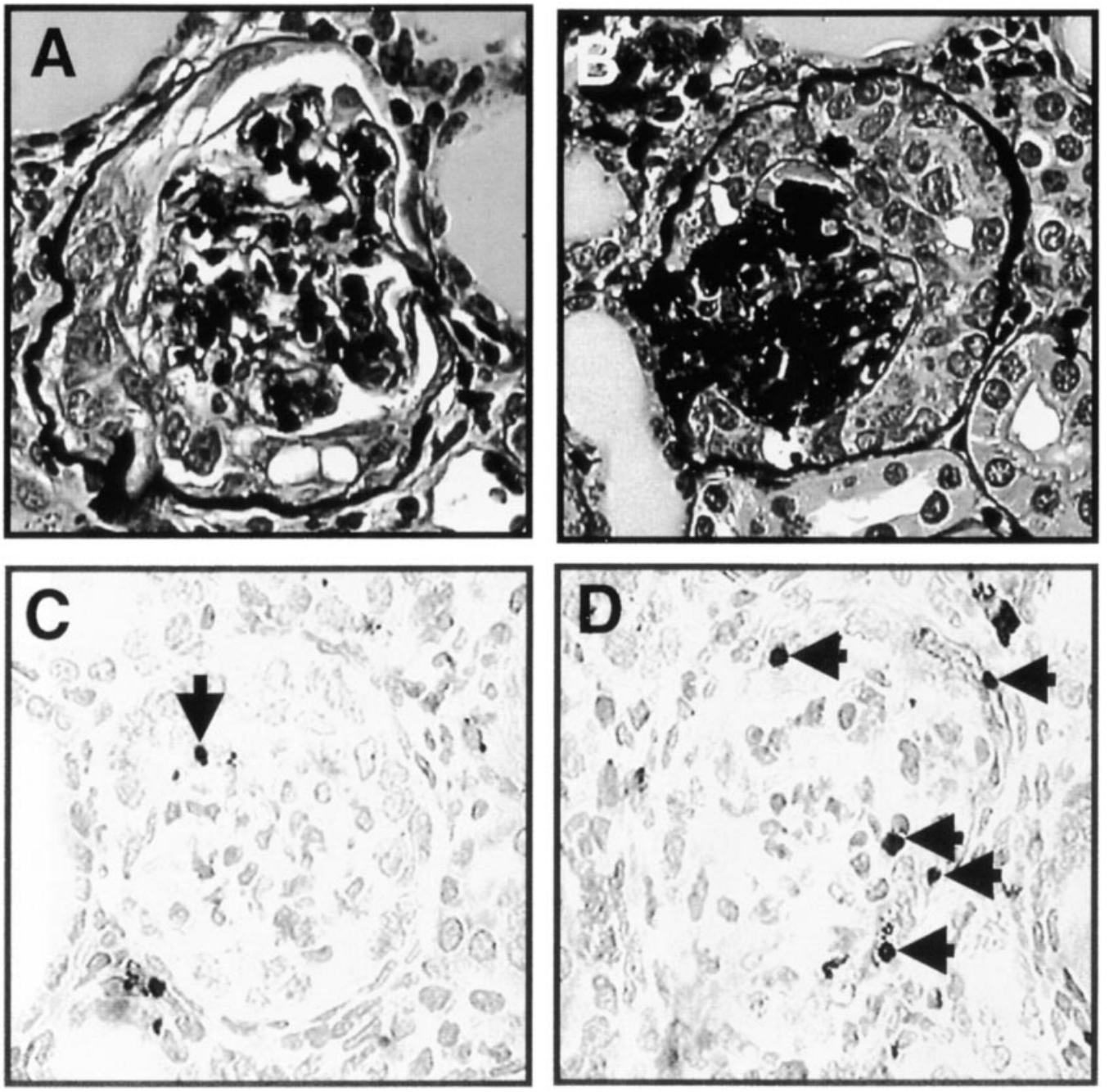

Fig. 6. Silver staining. There was an increase in silver staining at day 14 in nephritic p21−/− mice (*B*) compared with p21+/+ mice (*A*). (*C* and *D*) TUNEL staining. TUNEL staining, a marker of apoptosis, was increased at day 14 in nephritic p21−/− mice (D) compared with p21+/+ mice (C).

companied by increased DNA synthesis [20]. In this study, we also showed that DNA synthesis and proliferation of VECs were associated with the loss of WT-1 staining, a marker of differentiated VECs. Taken together, these data suggest that p21 is required to maintain the terminally differentiated VEC phenotype and support the idea that in disease, the loss of p21 is associated with a dedifferentiated VEC phenotype, which can readily proliferate in response to injury.

By light microscopy, proliferating VECs in this study often formed two or more layers of cells in Bowman's space, sometimes resembling glomerular crescents. Indeed, some have defined crescents as consisting of two or more layers of cells, and most studies of the mecha-

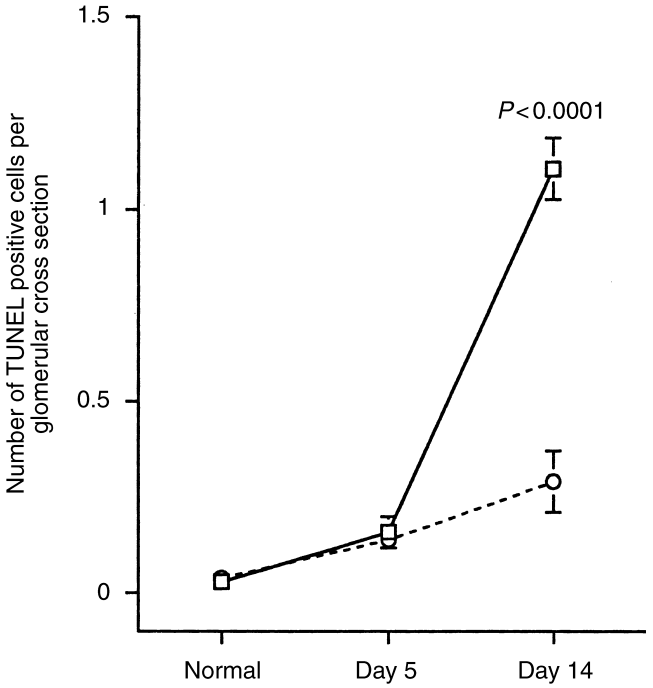

Fig. 7. Quantitation of TUNEL staining. There was a statistically significant increase in TUNEL staining in p21−/− mice (□) at day 14 compared with controls (p21+/+; ○).

nisms of crescent formation have been done in rodent nephrotoxic nephritis models such as this one [reviewed in 41]. However, current evidence suggests that crescents are composed predominantly of proliferating parietal VECs, macrophages, and fibroblasts, the latter two cells entering Bowman's space through disruptions in the glomerular basement membrane and Bowman's capsule [42]. Moreover, the mechanisms that underlie crescent formation involve cell-mediated rather than humoral immunity and lead to classic features of a delayed hypersensitivity reaction, including macrophage infiltration, T-cell localization, and fibrin deposition [41, 42]. In our study, the development of cell multilayers in Bowman's space was not associated with identifiable T cells, macrophages and fibrin deposits that may be due to the absence of gaps in the glomerular basement membrane or Bowman's capsule by light or electron microscopy, as has been shown previously [43, 44]. In this study, we did not measure differences in the balance between Th1 and Th2 responses in p21−/− and p21+/+ mice.

Although available markers do not permit the identity of the proliferating cells as parietal or visceral VECs in this experimental model to be established with certainty, their localization and morphology in nephritic p21−/− mice strongly suggest they are primarily visceral rather than parietal VEC associated with crescents. In contrast, there is low-grade proliferation of both visceral and parietal glomerular epithelial cells in nephritic p21+/+ mice. Thus, we believe that this phenomenon we are describing is a new type of glomerular response to injury representing marked proliferation of visceral VECs facilitated by the absence of p21. Although perhaps less relevant to crescentic glomerulonephritis, it exhibits features seen in the glomerular lesions described in collapsing glomerulopathy and HIV nephropathy [45, 46]. In addition to the possible relevance of these findings to human glomerular lesions, the observations reported are clearly central to understanding the spectrum of responses of the VEC injury and the factors that modulate them.

The mechanisms underlying VEC proliferation were not examined in this study. There are no reports of antibody alone directly causing glomerular cell proliferation, and this model is complement independent. Growth factors may have been increased or released following glomerular cell injury in this model. Our data do not support a direct role of infiltrating cells in this process.

Studies have shown that the cyclin kinase inhibitor p21 also has different roles in apoptosis in specific cell lineages. Thus, p21 is not required for apoptosis in certain nonrenal cells [47], but protects myocytes from apoptosis [48]. In this study, we showed that apoptosis was not detected in normal p21−/− kidneys and was not increased in p21−/− mice at day 5 of glomerulonephritis. There was a small but significant increase in apoptosis at day 14 of glomerulonephritis in p21−/− mice compared with p21+/+ mice. These results differ, therefore, from the marked increase in apoptosis in tubular epithelial cells following nonimmune mediated tubulotoxic injury [49] and suggest that the role for p21 in apoptosis *in vivo* may be cell-type or injury-type specific. In this study, we did not examine heterozygotes p21+/− mice, and one can only speculate that there may have been a gene "dose response" and that the injury would be milder than p21−/− mice. Our findings indicate that the increased VEC number observed in this model was not due to a decrease in the rate of cell removal by apoptosis. The results in this study also show that specific cyclin kinase inhibitors modulate the glomerular response to injury differently. Thus, in contrast to p21−/− mice, nephritic p27−/− mice have a marked increase in apoptosis that was in excess of the increase in proliferation [22].

In summary, this study shows that p21 is not required for normal glomerular development and VEC differentiation. However, p21 is required to maintain mature VECs in a differentiated phenotype. Following immune injury, the loss of p21 is associated with re-engagement of the cell cycle by VECs and the development of marked proliferation and glomerulosclerosis.

ACKNOWLEDGMENTS

This work was supported by National Institutes of Health grants (DK 52121, DK51096, DK34198) and a George M. O'Brien Kidney

Reseach Center Award (DK47659). Y.-G.K. was supported by Samsung Medical Center, Sungkyunkwan University, Seoul, Korea.

Reprint requests to Stuart J. Shankland, M.D., University of Washington Medical Center, Division of Nephrology, Box 356521, 1959 NE Pacific Avenue, Seattle, Washington 98195-6521, USA.
E-mail: stuartjs@u.washington.edu

APPENDIX

Abbreviations used in this article are: bFGF, basic fibroblast growth factor; BrdU, bromodeoxyuridine; CDK, cyclin dependent kinase; CKI, cyclin kinase inhibitor; DAB, diaminobenzidine; p21, $p21^{WAF1,CIP1}$; PCNA, proliferating cell nuclear antigen; PHN, passive Heymann nephritis; TdT, terminal deoxynucleotidyl transferase; TMA, thrombotic microangiopathy; TUNEL, terminal deoxytransferase uridine triphosphate nick end-labeling; VEC, visceral glomerular epithelial cell (podocyte); WT-1, Wilms' tumor-1 gene.

REFERENCES

1. Johnson RJ: The glomerular response to injury: Progression or resolution? *Kidney Int* 45:1769–1782, 1994
2. Kriz W: Progressive renal failure-inability of podocytes to replicate and the consequences for development of glomerulosclerosis. *Nephrol Dial Transplant* 11:1738–1742, 1996
3. Rennke HG: How does glomerular epithelial cell injury contribute to progressive glomerular damage? *Kidney Int* 45:S58–S63, 1994
4. D'Agati V: The many masks of focal segmental glomerulosclerosis. *Kidney Int* 46:1223–1241, 1994
5. Pardee AB: G1 events and regulation of cell proliferation. *Science* 246:603–608, 1989
6. Sherr CJ: Mammalian G1 cyclins. *Cell* 73:1059–1065, 1993
7. Sherr CJ: G1 phase progression: Cycling on cue. *Cell* 79:551–555, 1994
8. Sherr CJ, Roberts JM: Inhibitors of mammalian G1 cyclin-dependent kinases. *Genes Dev* 9:1149–1163, 1995
9. Harper JW, Adami GR, Wei N, Keyomarsi K, Elledge J: The p21 cdk-interacting protein Cip1 is a potent inhibitor of G1 cyclin-dependent kinases. *Cell* 75:805–816, 1993
10. Harper JW, Elledge SJ, Keyomarsi K, Dynlacht B, Tsai L, Zhang P, Dobrowolski S, Bai C, Connell-Crowley L, Swindell E, Fox MP, Wei N: Inhibition of cyclin dependent kinases by p21. *Mol Biol Cell* 6:387–400, 1995
11. El-Deiry WS, Tokino T, Velculescu VE, Levy DB, Parsons R, Trent JM, Lin D, Mercer WE, Kinzler KW, Vogelstein B: p21WAF1, a potential mediator of p53 tumor suppression. *Cell* 75:817–825, 1993
12. Noda A, Ning Y, Venable SF, Pereira-Smiths OM, Smith JR: Cloning of senescent cell-derived inhibitors of DNA synthesis using expression vectors. *Exp Cell Res* 211:90–98, 1994
13. Polyak K, Kato J, Solomon MJ, Sherr CJ, Massague J, Roberts JM, Koff A: p27kip1, a cyclin-Cdk inhibitor, links transforming growth factor-β and contact inhibition to cell cycle arrest. *Genes Dev* 8:9–22, 1994
14. Polyak K, Lee M-H, Erdjument-Bromage H, Koff A, Roberts JM, Tempst P, Massague J: Cloning of p27Kip1, a cyclin-dependent kinase inhibitor and potential mediator of extracellular antimitogenic signals. *Cell* 78:59–66, 1994
15. Zhang P, Liegeois NJ, Wong C, Finegold M, Hou H, Thompson JC, Silverman A, Harper JW, Depinho RA, Elledge SJ: Altered cell differentiation and proliferation in mice lacking p57Kip2 indicates a role in Beckwith-Wiedermann syndrome. *Nature* 387:151–158, 1997
16. Chen IT, Akamatsu M, Smith ML, Lung F, Duba D, Roleer PP, Fornace AJ Jr: Charaterization of p21 Cip1/Waf1 peptide domains required for cyclin E/CDK2 and PCNA interaction. *Oncogene* 12:595–607, 1996
17. Chen J, Peters R, Saha P, Lee P, Theodoras A, Pagano M, Wagner G, Dutta A: A 39 amino acid fragment of the cell cycle regulator p21 is sufficient to bind PCNA and partially inhibit DNA replication in vivo. *Nucleic Acid Res* 24:1727–1733, 1996
18. Zhang H, Xiong Y, Beach D: Proliferating cell nuclear antigen and p21 are components of multiple cell cycle kinase complexes. *Mol Biol Cell* 4:897–906, 1993
19. Parker SB, Eichele G, Zhang P, Rawls A, Sands AT, Bradley A, Olson EN, Harper JW, Elledge SJ: p53-Independent expression of p21Cip1 in muscle and other terminally differentiating cells. *Science* 267:1024–1027, 1995
20. Shankland SJ, Floege J, Thomas SE, Nangaku M, Hugo C, Pippin J, Henne K, Hockenberry DM, Johnson RJ, Couser WG: Cyclin kinase inhibitors are increased during experimental membranous nephropathy: Potential role in limiting glomerular epithelial cell proliferation in vivo. *Kidney Int* 52:404–413, 1997
21. Brugarolas J, Chandrasekaran C, Gordon JI, Beach D, Jacks T, Hannon GJ: Radiation-induced cell cycle arrest compromised by p21-deficiency. *Nature* 377:552–557, 1995
22. Ophascharoensuk V, Fero ML, Hughes J, Roberts JM, Shankland SJ: The cyclin-kinase inhibitor $p27^{Kip1}$ safegaurds against inflammatory injury. *Nat Med* 4:575–580, 1998
23. Floege J, Alpers CE, Sage EH, Pritzl P, Gordon K, Johnson RJ, Couser WG: Markers of complement-dependent and complement-independent glomerular visceral epithelial cell injury in vivo. *Lab Invest* 67:486–497, 1992
24. Shankland SJ, Pippin J, Pichler RH, Gordon KL, Friedman S, Gold LI, Johnson RJ, Couser WG: Differential expression of transforming growth factor-β isoforms and receptors in experimental membranous nephropathy. *Kidney Int* 50:116–124, 1996
25. Hugo C, Nangaku M, Shankland SJ, Pichler RH, Gordon KL, Amieva MR, Couser WG, Furthmayr H, Johnson RJ: The plasma membrane-actin linking protein, ezrin, is a glomerular epithelial cell marker in glomerulogenesis, in the adult kidney and in glomerular injury. *Kidney Int* 54:1934–1944, 1998
26. Mundlos S, Pelletier J, Darveau A, Bachmann M, Winterpacht A, Zabel B: Nuclear localization of the protein encoded by the Wilms' tumor gene WT1 in embryonic and adult tissues. *Development* 119:1329–1341, 1993
27. Salant DJ, Darby C, Couser WG: Experimental membranous glomerulonephritis in rats. *J Clin Invest* 66:71–81, 1980
28. Baker AJ, Mooney A, Hughes J, Lombardi D, Johnson RJ, Savill J: Mesangial cell apoptosis: The major mechanism for resolution of glomerular hypercellularity in experimental mesangial proliferative nephritis. *J Clin Invest* 94:2105–2116, 1994
29. Waga S, Hannon GJ, Beach D, Stillman B: The p21 inhibitor of cyclin-dependent kinases controls DNA replication by interaction with PCNA. *Nature* 369:574–578, 1994
30. Terada Y, Yamada T, Nakashima O, Tamamori M, Ito H, Sasaki S, Marumo F: Overexpression of cell cycle inhibitors (p16INK4 and p21Cip1) and cyclin D1 using adenovirus vectors regulates proliferation of rat mesangial cells. *J Am Soc Nephrol* 8:51–60, 1997
31. Nakanishi M, Adami GR, Robetorye RS, Noda A, Venable SF, Dimitrov D, Pereira-Smith OM, Smith JR: Exit from Go and entry into the cell cycle of cells expressing p21Sid1 antisense RNA. *Proc Natl Acad Sci USA* 92:4352–4356, 1995
32. Missero C, Di Cunto F, Kiyokawa H, Koff A, GPD: The absence of p21 (Cip1/WAF1) alters keratinocyte growth and differentiation and promotes ras-tumor progression. *Genes Dev* 10:3065–3075, 1996
33. Gartel AL, Serfas MS, Gartel M, Goufman E, Wu GS, El-Deiry WS, Tyner AL: p21 (WAF1/CIP1) expression is induced in newly nondividing cells in diverse epithelia and during differentiation of the Caco-2 intestinal cell line. *Exp Cell Res* 227:171–181, 1996
34. Missero C, Calautti E, Eckner R, Chin J, Tsai LH, Livingston DM, Dotto GP: Involvement of the cell-cycle inhibitor Cip1/WAF1 and the E1A-associated p300 protein in terminal differentiation. *Proc Natl Acad Sci USA* 92:5451–5455, 1995
35. Halevy O, Novitch BG, Spicer DB, Skapek SX, Rhee J, Hannon GJ, Beach D, Lassar AB: Correlation of terminal cell cycle arrest of skeletal muscle with induction of p21 by myoD. *Science* 267:1018–1021, 1995
36. Steinman RA, Hoffman B, Iro A, Guillouf C, Lieberman DA, El-Houseini ME: Induction of p21 (WAF1/CIP1) during differentiation. *Oncogene* 9:3389–3396, 1994

37. Saxen L: *Organogenesis of the Kidney.* Cambridge, Cambridge University Press, 1987
38. Deng C, Zhang P, Harper JW, Elledge SJ, Leder P: Mice lacking p21 (Cip1/WAF1) undergo normal development, but are defective in G1 checkpoint control. *Cell* 82:675–684, 1995
39. Coombs HL, Shankland SJ, Setzer SV, Hudkins KL, Alpers CE: Expression of the cyclin kinase inhibitor, $p27^{kip1}$, in developing and mature human kidney. *Kidney Int* 53:892–896, 1998
40. Kriz W, Hahnel B, Rosener S, Elger M: Long-term treatment of rats with FGF-2 results in focal segmental glomerulosclerosis. *Kidney Int* 48:1435–1450, 1995
41. Atkins RC, Nikolic-Paterson DJ, Song Q, Lan HY: Modulators of crescentic glomerulonephritis. *J Am Soc Nephrol* 7:2271–2278, 1996
42. Wiggens RC, Holzman LB, Legault DJ: Glomerular inflammation and crescent formation, in *Immunological Renal Diseases*, edited by Neilson EG, Couser WG, Philadelphia, Lippincott-Raven, 1997
43. Lan HY, Nikoloc-Paterson DJ, Atkins RC: Involvement of activated periglomerular leukocytes in the rupture of Bowman's capsule and glomerular crescent progression in experimental glomerulonephritis. *Lab Invest* 67:743–751, 1992
44. Boucher A, Droz D, Adafer E, Noel LH: Relationship between the integrity of Bowman's capsule and the composition of cellular crescents in human crescentic glomerulonephritis. *Lab Invest* 56:526–533, 1987
45. Detwiler RK, Falk RJ, Hogan SL, Jennette JC: Collapsing glomerulopathy: A clinically and pathologically distinct variant of focal segmental glomerulosclerosis. *Kidney Int* 45:1416–1424, 1994
46. Valeri A, Barisoni L, Appel GB, Seigle R, D'Agati V: Idiopathic collapsing focal glomerulosclerosis: A cinicopathologic study. *Kidney Int* 50:1734–1746, 1996
47. Freemerman AJ, Vrana JA, Tombes RM, Jiang H, Chellapan SP, Fisher PB, SG: Effects of antisense p21 (WAF1/Cip1/MDA6) expression on the induction of differentiation and drug-mediated apoptosis in human myeloid leukemia cells (HL-60). *Leukemia* 11:504–513, 1997
48. Wang J, Walsh K: Resistance to apoptosis conferred by Cdk inhibitors during myocyte differentiation. *Science* 273:359–361, 1996
49. Megyesi J, Safirstein RL, Price PM: Induction of p21 (WAF1/Cip1/SDI1) in kidney tubule cells affects the course of cisplatin-induced acute renal failure. *J Clin Invest* 101:777–782, 1998